Bone 146 (2021) 115884

Contents lists available at ScienceDirect

Bone

journal homepage: www.elsevier.com/locate/bone

Early B-cell Factor1 (Ebf1) promotes early osteoblast differentiation but suppresses osteoblast function

Vappu Nieminen-Pihala [a], Kati Tarkkonen [a,1], Julius Laine [a,4], Petri Rummukainen [a], Lauri Saastamoinen [a,2], Kenichi Nagano [b,3], Roland Baron [b], Riku Kiviranta [a,c,*]

[a] Institute of Biomedicine, University of Turku, Turku, Finland
[b] Department of Oral Medicine, Infection and Immunity, Harvard School of Dental Medicine, Harvard University, Boston, MA, USA
[c] Department of Endocrinology, Division of Medicine, University of Turku and Turku University Hospital, Turku, Finland

ARTICLE INFO

Keywords:
Ebf1
Osteoblast
Osterix
Osteoblast differentiation
Bone formation
Transcriptional regulation
Conditional knockout mouse model

ABSTRACT

Early B cell factor 1 (Ebf1) is a transcription factor that regulates B cell, neuronal cell and adipocyte differentiation. We and others have shown that Ebf1 is expressed in osteoblasts and that global deletion of Ebf1 results in increased bone formation *in vivo*. However, as Ebf1 is expressed in multiple tissues and cell types, it has remained unclear, which of the phenotypic changes in bone are derived from bone cells. The aim of this study was to determine the cell-autonomous and differentiation stage-specific roles of Ebf1 in osteoblasts.

In vitro, haploinsufficient $Ebf1^{+/-}$ calvarial cells showed impaired osteoblastic differentiation indicated by lower alkaline phosphatase (ALP) activity and reduced mRNA expression of osteoblastic genes, while overexpression of Ebf1 in wild type mouse calvarial cells led to enhanced osteoblast differentiation with increased expression of Osterix (Osx). We identified a putative Ebf1 binding site in the Osterix promoter by ChIP assay in MC3T3-E1 osteoblasts and showed that Ebf1 was able to activate Osx-luc reporter construct that included this Ebf1 binding site, suggesting that Ebf1 indeed regulates osteoblast differentiation by inducing Osterix expression.

To reconcile our previous data and that of others with our novel findings, we hypothesized that Ebf1 could have a dual role in osteoblast differentiation promoting early but inhibiting late stages of differentiation and osteoblast function. To test this hypothesis *in vivo*, we generated conditional Ebf1 knockout mice, in which Ebf1 deletion was targeted to early or late osteoblasts by crossing $Ebf1^{fl/fl}$ mice with Osx- or Osteocalcin (hOC)-Cre mouse lines, respectively. Deletion of Ebf1 in early $Ebf1_{\overline{Osx}}^{\overline{/-}}$ osteoblasts resulted in significantly increased bone volume and trabecular number at 12 weeks by μCT analysis, while $Ebf1_{\overline{hOC}}^{\overline{/-}}$ mice did not have a bone phenotype.

To conclude, our data demonstrate that Ebf1 promotes early osteoblast differentiation by regulating Osterix expression. However, Ebf1 inhibits bone accrual in the Osterix expressing osteoblasts *in vivo* but it is redundant in the maintenance of mature osteoblast function.

1. Introduction

Bone tissue is remodelled in a continuous cycle of bone resorption by osteoclasts and bone formation by osteoblasts. Constant remodeling maintains the structural integrity of the bone tissue and participates in calcium and phosphate homeostasis. Osteoblasts originate from mesenchymal stromal cells (MSCs), common progenitors for all the mesenchymal cell types such as chondrocytes, myoblasts and adipocytes. The differentiation fate of mesenchymal stromal cells into mature cells is determined by lineage-specific transcription factors [1]. Runt-related transcription factor 2 (Runx2) [2] and Osterix (Osx) [3] are key determinants of osteoblast differentiation and bone development as shown in studies, in which the lack of either Runx2 or Osterix resulted in total absence of osteoblasts and bone [4,5].

* Corresponding author at: Institute of Biomedicine, University of Turku, FI-20520 Turku, Finland.
E-mail address: riku.kiviranta@utu.fi (R. Kiviranta).
[1] Present address: Orion Pharma, Turku, Finland.
[2] Present address: 2BScientific Limited, Oxfordshire, England.
[3] Present address: Department of Oral Pathology, Institute of Biomedical Sciences, Nagasaki University, 1-7-1 Sakamoto, Nagasaki-city, Nagasaki 852-8588, Japan.
[4] Present address: Heltti, Helsinki, Finland.

https://doi.org/10.1016/j.bone.2021.115884
Received 7 July 2020; Received in revised form 22 December 2020; Accepted 9 February 2021
Available online 12 February 2021
8756-3282/© 2021 The Authors. Published by Elsevier Inc. This is an open access article under the CC BY-NC-ND license (http://creativecommons.org/licenses/by-nc-nd/4.0/).

Early B-cell factor (Ebf1) is a zinc-knuckle containing transcription factor that regulates differentiation of multiple cell types including B-cells [6], adipocytes [7] and neuronal cells [8]. We and others have shown that Ebf1 also plays a role in the regulation of bone metabolism. Ebf1 is expressed in osteoblasts and global deletion of Ebf1 results in increased bone formation *in vivo* [9,10]. However, as Ebf1 is expressed in multiple tissues including central nervous system, results acquired from global Ebf1 knockout models have their limitations; changes in the skeletal development might arise for example from defects in neuronal cell function. Conversely, overexpression of Ebf1 targeted to mature osteoblasts results in impaired bone formation implicating Ebf1 as a negative regulator of osteoblast function [10].

There are also studies suggesting Ebf1 has a very minor role in osteoblast differentiation *in vivo* [11,12]. Zee et al. reported that targeting Ebf1 deletion to osteoblast lineage cells by Runx2-Cre had no effect on the osteoblast differentiation or bone accrual [11], while Seike et al. showed that Prrx1-Cre driven deletion of Ebf1 in limb bud mesenchymal cells caused no bone abnormalities [13]. Recently Derecka et al. in turn presented how Prrx1-Cre driven deletion of Ebf1 led to increased bone volume [14]. However, the age of the mice and therefore the current bone remodeling status, as well as promoters used to drive Cre recombinase expression vary greatly between studies, making their comparison difficult. Thus, the specific role of Ebf1 in osteoblast differentiation and function still remains unclear.

To investigate the differentiation stage-specific role of Ebf1 in cells committed to the osteoblast lineage, we generated osteoblast-targeted Ebf1 knockout mice. In our models Ebf1 deletion was targeted to early or late osteoblasts using Osterix-Cre (Osx-Cre) or human Osteocalcin promoter driven Cre (hOC-Cre) mouse lines, respectively. The phenotypes were analyzed at 12 weeks and 24 weeks. Deletion of Ebf1 in early osteoblasts in $Ebf1^{-/-}_{Osx}$ mice resulted in significantly increased bone volume at the age of 12 weeks due to increased osteoblast function while $Ebf1^{-/-}_{hOC}$ mice did not have a bone phenotype. Overexpression of Ebf1 in mouse calvarial cells *in vitro* led to enhanced osteoblast differentiation with increased expression of Osterix, whereas osteoblast differentiation in $Ebf1^{-/-}$ cultures was impaired. We also identified a putative Ebf1 binding site in Osterix promoter by ChIP assay in MC3T3-E1 osteoblasts. Ebf1 was also able to activate Osx-luc in the luciferase assay indicating that the putative site was functional. Our data suggest that Ebf1 promotes early osteoblast differentiation, *via* inducing Osterix expression, but inhibits osteoblast function in committed Osterix-expressing osteoblasts.

2. Methods

2.1. Experimental animals

$Ebf1^{+/-}$ mice were provided by Dr. J. Hagman (National Jewish Health, Denver, CO) and Dr. R. Grosschedl (Max Planck Institute of Immunobiology and Epigenetics, Freiburg, Germany; [15]), and maintained on C57BL background. $Ebf1^{fl/fl}$ mice were also provided by Dr. J. Hagman and have been described previously [16]. To create conditional, osteoblast specific Ebf1 knockout mice, we crossed $Ebf1^{fl/fl}$ mice with Osx- or hOC-Cre mouse lines, respectively. Osx-Cre and hOC-Cre transgenic mice have been described previously [17,18]. Since Osx-Cre is known to have an effect on the bone phenotype [19], Cre positive $Ebf1^{+/+}$ Osx-Cre + mice were used as controls. We did not observe any bone phenotype in hOC-Cre mice (data not shown), therefore Cre negative $Ebf1^{fl/fl}$ hOC-Cre - mice were used as controls. Samples were collected from male and female mice at 12 weeks and 24 weeks of age. Data presented in the main text are from male mice. Data from female mice are included in the supplemental data.

The animals were housed in cages under standard laboratory conditions (temperature 22 °C, light from 6:00 AM to 6:00 PM.) Water and soy-free food pellets were available *ad libitum*, excluding a four-hour fasting period before euthanization.

2.2. Measurement of gene expression

Total RNA from cell cultures was isolated using RNeasy mini kit (QIAGEN) or NucleoSpin RNA Plus (Macherey-Nagel). cDNA was prepared with DyNAmo cDNA Synthesis Kit (Thermo Fisher) or Sensifast cDNA synthesis kit (BioLine). Quantitative real-time PCR (qPCR) was performed using iQ SYBR Green Supermix (Bio-Rad Laboratories) or Dynamo Flash SYBR Green qPCR Kit (ThermoFisher). The samples were run with Bio-Rad CFX96 qPCR system. The data was normalized using beta-actin or cyclophilin as an internal control and the results were analyzed by ΔΔCt-method. Primer sequences are provided upon request.

2.3. Plasmids

Plasmids for the reporter assay and overexpression assay, pCDNA3-Flag-Ebf1 and pMSCV-Flag-Ebf1 constructs [20], respectively, were a gift from Dr. E.D. Rosen. The Osx-Luc plasmid has been previously published [21].

2.4. Cell lines

HEK293T and 293T Phoenix cells were cultured and maintained in Dulbecco's Modified Eagle Medium (DMEM) with 1% penicillin/streptomycin and 10% heat-inactivated fetal bovine serum (iFBS). MC3T3-E1 cells were purchased from ATCC and cultured and maintained in α-minimal essential medium (α-MEM) 1% penicillin/streptomycin and 10% fetal bovine serum (FBS USA origin, Gibco).

2.5. Luciferase assay

For reporter assays, HEK293T cells were plated on 96-well plates and transfected with Osx-Luc reporter plasmid, pCDNA3-Flag-Ebf1 and pRL promoterless Renilla plasmid using Fugene 6 reagent (Invitrogen). Reporter activity was measured with the Dual Luciferase Reporter assay (Promega) 24–48 h after transfection and normalized for Renilla activity.

2.6. Chromatin immunoprecipitation

The chromatin immunoprecipitation (ChIP) protocol was modified from Östling et al. [22]. In short, MC3T3-E1 cells were cultured to subconfluence and cross-linked with a final concentration of 1% formaldehyde. Quenching was performed with a final concentration of 125 mM glycine. The cells were scraped, washed in PBS and resuspended in lysis buffer containing 1% SDS, 10 mM EDTA, 50 mM Tris-HCl and protease inhibitors (Complete, Roche). Fragmentation of the chromatin samples was performed by sonication with Bioruptor (Diagenode) to an approximate size of 500 bp. After chromatin shearing, the chromatin was diluted with IP-buffer containing 150 mM NaCl, 20 mM Tris-HCl and 1% Triton-X and protease inhibitors. Antibodies against mouse Ebf1 1C12 (Abnova, Everest) or mouse normal IgG (Santa Cruz) were added to samples and incubated overnight. Magnetic Dynabeads Protein A beads (Invitrogen) were used to harvest bound protein–chromatin complexes. After washing, cross-links were reversed by incubating the samples overnight at 65 °C. DNA was purified and subjected to qPCR analysis using Osterix promoter-specific primer sequences: 5′-gcccatattcctgtttcccacccg-3′ and 5′-tgctctgtctgtagggatccacc-3′ and with Dynamo Flash qPCR kit (Thermo-Fischer).

2.7. Histology and histomorphometry

The mice were injected with 20 mg/kg of Calcein (C0875, Sigma) and 40 mg/kg of Demeclocycline (D6140, Sigma) 9 and 2 days prior to sacrifice, respectively. For the microcomputed tomography (μCT) bones were stripped from soft tissues, and stored in 70% EtOH at +4C. For histomorphometry the right femurs were harvested and fixed in 70%

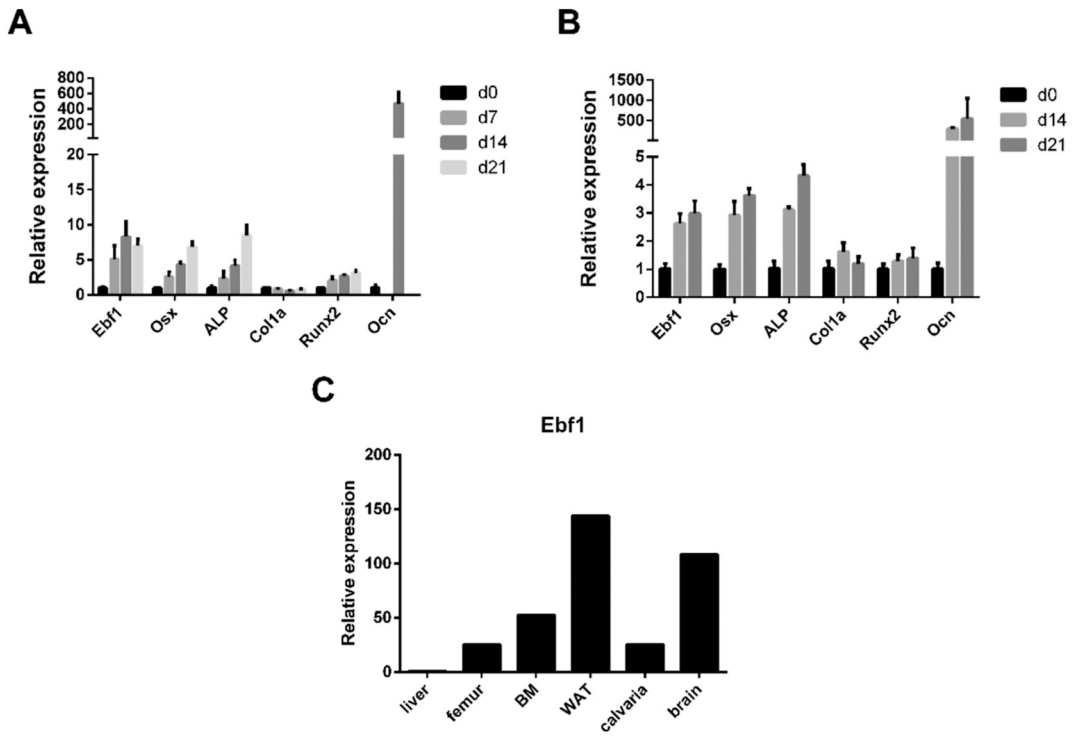

Fig. 1. Osteoblast specific gene mRNA expression in WT calvarial osteoblast culture (A) and in MC3T3-E1 osteoblast cell line (B). Ebf1 mRNA expression in WT mouse tissue panel samples of liver, femur, bone marrow (BM), white adipose tissue (WAT), calvaria and brain (C). Representative data from at least three independent experiments, triplicate wells in each (A&B).

ethanol for 3 days. The fixed bones were dehydrated with acetone and embedded in methylmethacrylate. Undecalcified 4-μm-thick sections were cut with hard tissue microtome (RM2255, Leica, Germany), deplastified and stained with Von Kossa method using the standard protocol to show the mineralized bone. Consecutive section was stained with 2% Toluidine Blue (pH 3.7) for the analysis of osteoblasts, osteoid and osteoclasts and next sections were left unstained for the analysis of fluorescence labeling.

The image capture and bone histomorphometric analysis were performed with the Nikon E800 microscope equipped with Olympus DP71 digital camera. The image capture was performed by using Olympus cellSens software under 20× magnification. The bone histomorphometric analysis was performed in the distal femur under 200× magnification in a 0.9 mm high x 1.3 mm wide region 200 μm away from the growth plate using OsteoMeasure analysis software (Osteometrics Inc., Decatur, GA, USA). The structural parameters [bone volume (BV/TV), trabecular thickness (Tb.Th), trabecular number (Tb.N) and trabecular separation (Tb.Sp)] were obtained by taking an average of 2 different measurement from consecutive sections. The structural, dynamic and cellular parameters were calculated and expressed according to the standardized nomenclature [23].

2.8. Microcomputed tomography

Femurs, tibias and vertebras were scanned and analyzed with SkyScan 1072 and SkyScan 1272 X-ray computed tomography (Bruker-microCT, Kontich, Belgium). A plastic holder was used to ensure immobilization and constant positioning of the sample. The parameters used for scanning (in air) were: cross-sectional pixel size 8.4 μm, X-ray tube voltage 72 kV, tube current 138 μA. The bones were rotated in 0.45°degree steps (total angle, 185.85°) and an internal 0.25 mm aluminum filter was applied for beam hardening. Cross-sectional images were reconstructed with NRecon 1.6.4.1 software (Bruker-microCT) as follows: dynamic range 0.014–0.130 attenuation coefficient units, beam hardening reduction 95% and ring artifact reduction level 9. CTan 1.10.10 software (Bruker-microCT) was used for analysis. For the analysis of the trabecular bone in the femur and tibia, a region of interest (ROI) excluding the cortical bone was defined 50 layers (488 μm) below the growth plate, for a total of 120 layers (1171 μm). Cortical bone was analyzed beginning from 4500 μm below the growth plate, for a total of 50 layers (488 μm). For the analysis of the trabecular bone in the fourth lumbar vertebrae, a ROI excluding the cortical bone was defined 30 layers (292 μm) above the distal growth plate and extending 100 layers (979 μm) proximally.

2.9. Primary osteoblast isolation and culture

Murine calvarial osteoblasts from mice less than 72 h old were collected by enzymatic digestion (0,1% collagenase (Roche) and 0,2% dispase (Sigma) in α -MEM, at +37C degrees). First fraction was discarded after 10 min incubation. Fractions 2–5 were collected each after 20 min digestion and pooled. Pooled cells were plated on 10 cm plates, one calvaria/plate in α -MEM (with 1% penicillin/streptomycin and 10% FBS). Media was changed the next day. During the expansion culture, donor pups were genotyped. Before reaching confluency, cells were used for cultures.

Cells for osteoblast differentiation were cultured on 6-well plates, at a seeding density of $1,5 * 10^{\wedge 5}$ cells/well or on 12-well plates at $4 * 10^{\wedge -4}$/well. At confluency (usually 3 days after seeding), osteoblast differentiation was induced with differentiation media (α-MEM, 10%FBS, 1% penicillin/streptomycin, 100 μg/ml ascorbic acid, 3 mM β-glycerol phosphate, 10 nM dexamethasone).

2.10. Retroviral overexpression cultures

293T Phoenix retroviral packaging cells were plated on T75-bottles, at a seeding density of $3 * 10^{\wedge 6}$/bottle, 24 h prior to transfection. The cells were transfected at approximately 50% confluency with either puromycin resistant retroviral control vector pMSCV or pMSCV-Ebf1 [20], and virus supernatants were harvested at 48 h and 72 h post

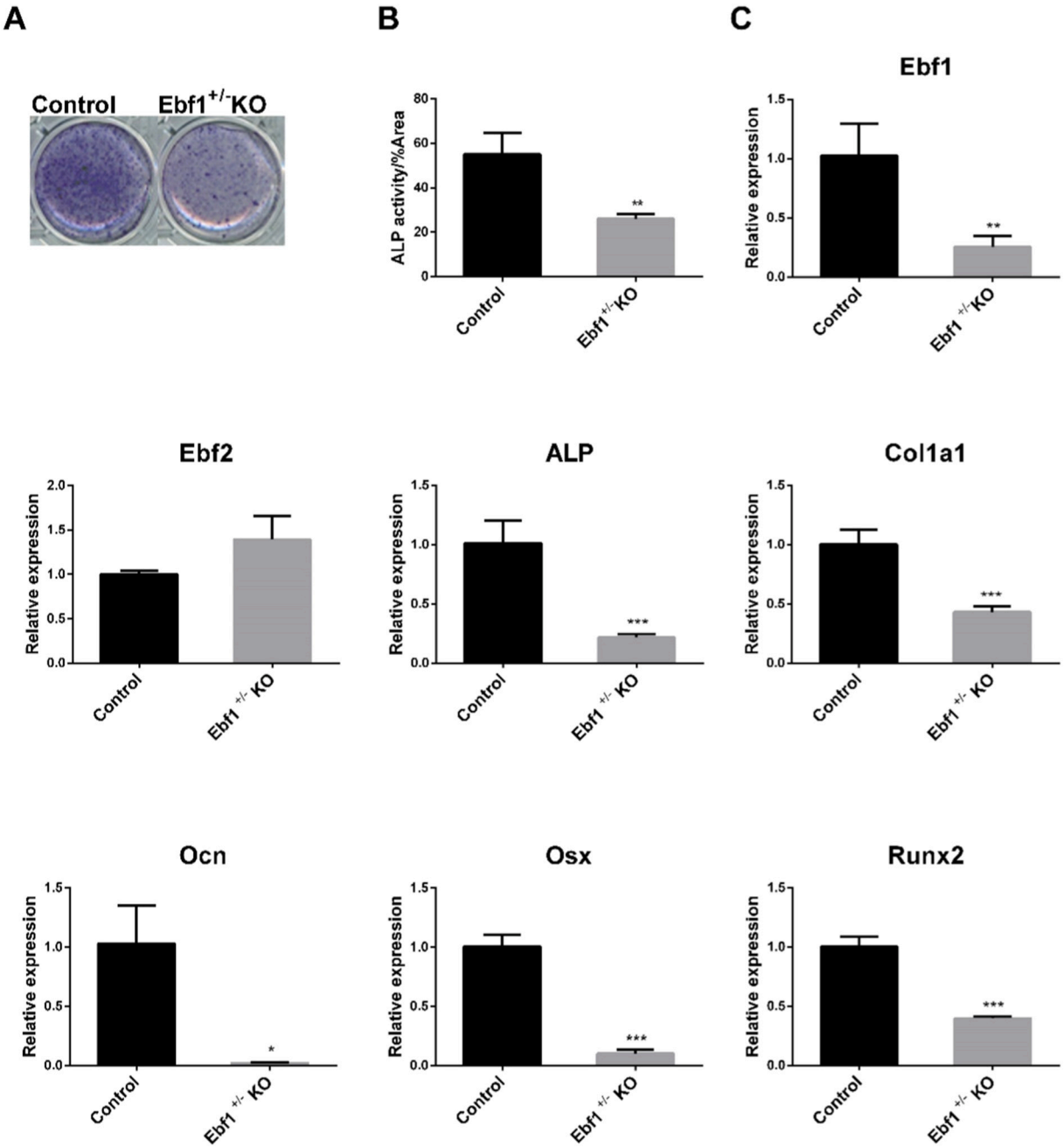

Fig. 2. Haploinsufficient Ebf1$^{+/-}$ calvarial cells in osteoblast culture, timepoint d14. ALP staining of primary osteoblast culture (A) and image analysis on the % of ALP activity (B). Gene mRNA expression measured by qRT-PCR. Bone related transcription factors (C) as well as bone matrix markers were significantly decreased in Ebf1$^{+/-}$ calvarial cells, except for Ebf2. Representative data from at least three independent experiments, triplicate wells in each. * $P < 0.05$; **, $P < 0.01$; ***, $P < 0.001$.

transfection.

Target cells (primary mouse calvarial cells) were plated on T75-bottles, at a seeding density of 6.5 * $10^{\wedge}5$/bottle, 24 h prior to infection. Target cells were infected at approx. 50% confluency for a minimum of 3 h. Polybrene was added to the viral media prior to infection, at a final concentration of 4 μg/ml. One volume of normal growth media was then added to the viral media. The infection was repeated 24 h later. Puromycin selection was started 48 h after the first infection.

Cells surviving the selection were expanded in culture, maintaining the confluence below 80% at all times. For osteoblast induction, cells were plated on 12-well plates at a seeding density of 4,0 * $10^{\wedge}4$/well. Osteogenic stimulation was started once the wells had reached confluence, usually 3 days after the seeding.

2.11. Histochemical analysis of primary osteoblast cultures

For alkaline phosphatase and Von Kossa stainings, cells were fixed with 3.7% formalin for 15 min, washed twice with water, and incubated with alkaline phosphatase staining solution (Naphtol AS phosphate, Fast blue RR salt, *N*,*N*-dimethylformamide, all from Sigma) for 45 min at room temperature. After three subsequent washes with water, wells were stained with 2.5% silver nitrate for 30 min at room temperature.

2.12. Statistical analysis

All the *in vitro* experiments have been repeated at least three or more times. Results are presented as mean ± SD. Statistical analysis was

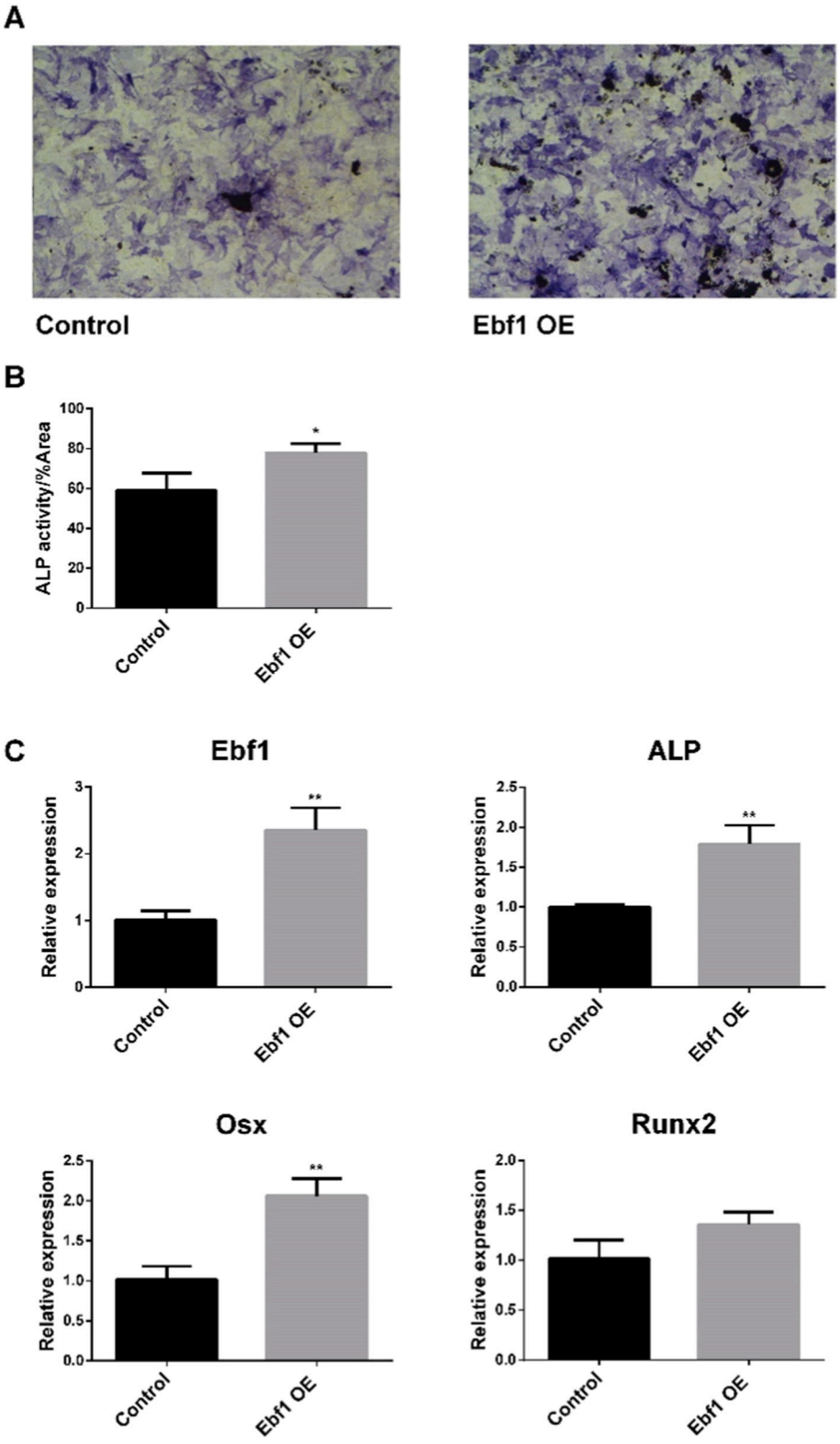

Fig. 3. Overexpression of Ebf1 in calvarial osteoblast culture, timepoint d14. Alkaline phosphatase (ALP) staining of primary osteoblasts (A) shows a clear difference between control and Ebf1 overexpression (Ebf1 OE) as does image analysis on the % of ALP activity (B). mRNA expression of Ebf1, ALP, Osx and Runx2 measured by qRT-PCR (C). Representative data from at least three independent experiments, triplicate wells in each. * $P < 0.05$; **, $P < 0.01$; ***, $P < 0.001$.

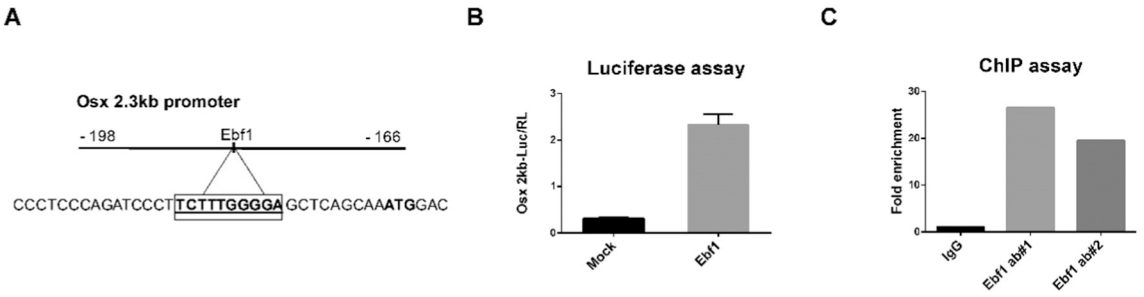

Fig. 4. A putative Ebf1 binding site (A) in the Osterix (Osx) promoter activated Osx-luc significantly in the luciferase assay (B). Ebf1 also bound to this site in ChIP assay (C). Representative data from at least three independent experiments.

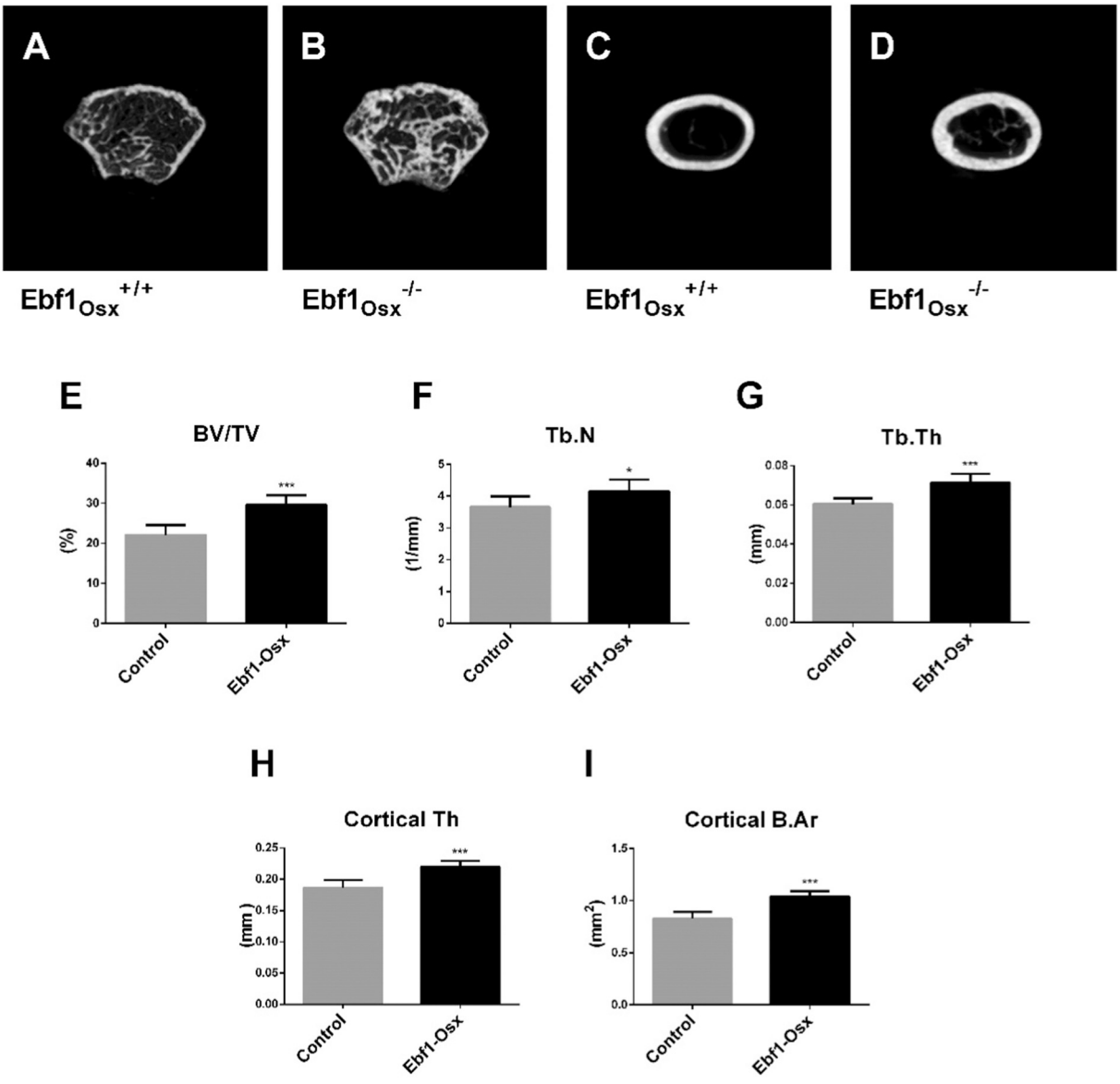

Fig. 5. Results of the femoral μCT-analysis of $Ebf1_{Osx}$ mice. 3D rendered representation of the trabecular region of interest in $Ebf1^{+/+}_{Osx}$ mice (A) and $Ebf1^{-/-}_{Osx}$ mice (B) and cortical region of interest in $Ebf1^{+/+}_{Osx}$ mice (C) and $Ebf1^{-/-}_{Osx}$ mice (D). Deletion of Ebf1 in early osteoblasts (12-week-old $Ebf1^{+/+}_{Osx}$ and $Ebf1^{-/-}_{Osx}$) resulted in significantly increased trabecular bone parameters (figs. E to G) and cortical bone parameters (figs. H and I). * $P < 0.05$; **, $P < 0.01$; ***, $P < 0.001$ $n = 7$ in $Ebf1^{+/+}_{Osx}$ mice, $n = 6$ in $Ebf1^{-/-}_{Osx}$ mice.

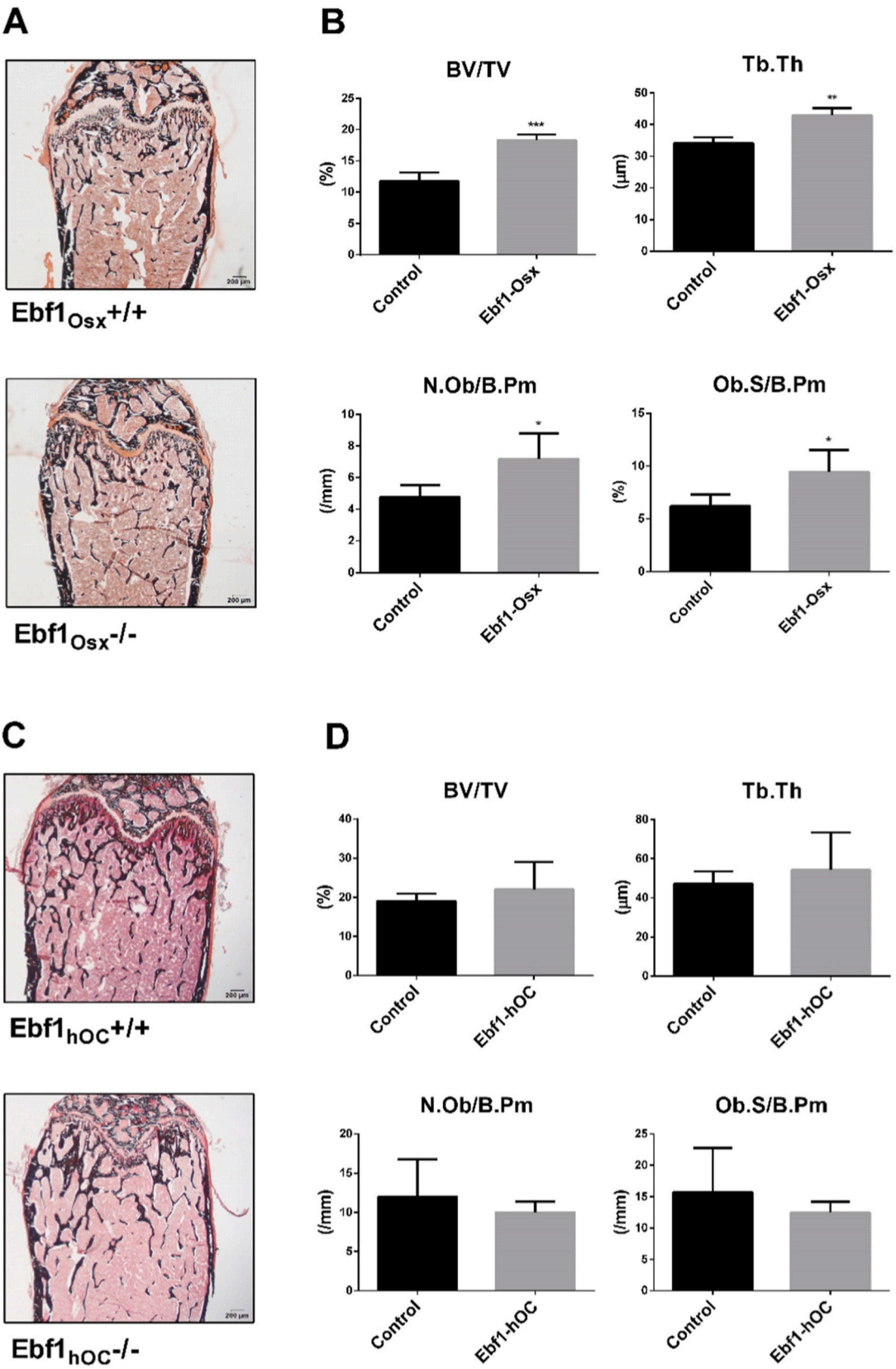

Fig. 6. Results of the femoral histomorphometric analysis. Von Kossa stained sections of $Ebf1_{Osx}^{+/+}$ and $Ebf1_{Osx}^{-/-}$ mice (A). Deletion of Ebf1 in early osteoblasts (12-week-old [illegible] $Ebf1_{hOC}^{-/-}$ mice (C). Deletion of Ebf1 in mature osteoblasts (12-week-old $Ebf1_{hOC}^{+/+}$and $Ebf1_{hOC}^{-/-}$) had no effect on trabecular bone parameters or osteoblast numbers (D) * $P < 0.05$; **, $P < 0.01$; ***, $P < 0.001$ $n = 5$ in all groups.

performed by two-tailed Student's *t*-test. *P*-values <0.05 were considered statistically significant.

3. Results

3.1. Heterozygous deletion of Ebf1 leads to impaired osteoblast differentiation

Our previous work and those of others suggest that Ebf1 is a negative regulator of osteoblast differentiation and bone formation [9,10]. The level of Ebf1 mRNA expression is in line with other osteoblast specific genes during osteoblast differentiation both in calvarial osteoblasts (Fig. 1-A) and in MC3T3-E1 osteoblastic cell line (Fig. 1-B) *in vitro*. However, Ebf1 is expressed in multiple tissues and cell types *in vivo* (Fig. 1-C).

Global deletion of Ebf1 results in severe developmental problems in multiple tissues that may influence the *in vivo* skeletal phenotype. The severe phenotype may even affect the *in vitro* phenotype of the primary calvarial cells extracted from the Ebf1$^{-/-}$ pups. To overcome these issues, we cultured calvarial cells from haploinsufficient Ebf1$^{+/-}$ newborn mice that do not exhibit any major developmental problems. In these cultures, Ebf1$^{+/-}$ calvarial cells formed less mineralized bone nodules and had lower ALP activity compared to control cells (Fig. 2, A-B). Ebf1 mRNA expression was significantly decreased in Ebf1$^{+/-}$ cells confirming that the haploinsufficiency was sufficient to reduce Ebf1 expression, while there was a modest non-significant increase in the expression of Ebf2 mRNA (Fig. 2-C). Impaired osteoblastic differentiation of Ebf1$^{+/-}$ cells was confirmed by significantly reduced mRNA expression of osteoblastic genes ALP, type I collagen (Col1a1) and osteocalcin (Ocn) (Fig. 2-C). Reduced Ebf1 expression also led to decreased mRNA levels of Runx2 and even more pronounced suppression of Osterix expression, which are both essential for osteoblast differentiation (Fig. 2-C). Based on our findings we hypothesized that Ebf1 could directly regulate Osterix expression.

3.2. Overexpression of Ebf1 enhances osteoblast differentiation

To test whether excess Ebf1 could induce osteoblast differentiation we overexpressed Ebf1 in primary calvarial osteoblasts *in vitro*. Overexpression of Ebf1 in osteoblast progenitors led to enhanced osteoblast differentiation demonstrated by increased ALP activity (Fig. 3, A-B) as well as in ALP mRNA expression. Interestingly, we observed that in contrast to Ebf1$^{+/-}$ calvarial cells, Ebf1 overexpression stimulated the expression of Osx but had no effect on Runx2 mRNA expression. (Fig. 3-C) Taken together these data led us to test whether Ebf1 could control early osteoblast differentiation by regulating Osterix expression.

3.3. Ebf1 induces Osterix expression directly by binding to the Osterix promoter

Osterix expression is regulated by multiple different growth factor signals in osteoblasts [24,25]. We first examined Osterix promoter and indeed identified a putative Ebf1 binding site in the proximal Osterix promoter (Fig. 4-A). Ebf1 also activated Osx-luc in the luciferase assay using a 2 kb promoter fragment in HEK293 T cells that included this putative binding site suggesting that the site was functional (Fig. 4-B). To confirm that Ebf1 indeed interacts with this site in osteoblastic cells we cultured MC3T3-E1 cells, that express Ebf1, and performed a chromatin immunoprecipitation on fixed and fragmented chromatin extracted from these cells with two different specific Ebf1 antibodies. Using qPCR with specific primers flanking the Ebf1 consensus site we found a robust enrichment of Ebf1 promoter signal with both of the antibodies compared to IgG control (Fig. 4-C). Taken together these data demonstrate that Ebf1 binds to the proximal Osterix promoter to induce its expression.

Table 1
Histomorphometric analysis of Ebf1$^{-/-}_{Osx}$ mice.

Parameter	Control	Ebf1$^{-/-}_{Osx}$
Tb.N [/mm]	3.45 ± 0.39	4.28 ± 0.30**
Tb.Sp [um]	259 ± 34.1	192 ± 14.9**
MAR [um/day]	1.79 ± 0.32	1.67 ± 0.25
BFR/BV [%/day]	4.47 ± 0.77	3.30 ± 0.82
Oc.S/B·Pm [%]	10.0 ± 1.63	10.7 ± 3.07
N.Oc/B·Pm [/mm]	4.08 ± 0.50	3.92 ± 1.16
OS/BS [%]	6.18 ± 2.76	7.19 ± 2.63
O·Th [um]	2.30 ± 0.41	2.91 ± 0.43

Data are mean ± SD.
$n = 5$ for Control and Ebf1$^{-/-}_{Osx}$.
** $P < 0.01$.

3.4. Deletion of Ebf1 in early committed osteoblasts results in increased bone mass

Homozygous Ebf1$^{-/-}$ mice develop a complex phenotype with low bone mass but increased trabecular bone formation. Moreover, due to the effects of Ebf1 deletion in other tissues such the brain the animals fail to thrive [9]. We reported that overexpression of Ebf1 in committed osteoblasts using Col1-2.3 kb promoter leads to increased number of osteoblasts but low bone mass due to decreased bone formation [10]. To determine the osteoblast-specific functions of Ebf1 at different stages of osteoblast differentiation we generated knockout mice, in which Ebf1 deletion was targeted to committed osteoblasts using Osx-Cre [17] (Ebf1$^{-/-}_{Osx}$ mice) and to mature osteoblast with hOC-Cre [18] (Ebf1$^{-/-}_{hOC}$ mice). Deletion was verified by a genomic PCR (Supplemental Fig. 1). Osx-Cre has later been found to be expressed also in the mouse olfactory bulb [26], which explains the faint deletion band expression in the brain. This however should not affect the bone phenotype.

Mice were analyzed at 12 and 24 weeks of age. Both male and female Ebf1$^{-/-}_{Osx}$ and Ebf1$^{-/-}_{hOC}$ mice had normal body weights and tibial lengths (Supplemental Fig. 2). We did not observe increased adiposity of the bone marrow reported by Hesslein et al. [9] in the analyzed histological sections of the Ebf1$^{-/-}_{Osx}$ male mice (Supplemental Fig. 3).

μCT analysis of the 12-week-old Ebf1$^{-/-}_{Osx}$ male mice femurs showed that the deletion of Ebf1 in early osteoblasts resulted in significantly elevated trabecular bone mass as demonstrated by a 30% increase in bone volume (BV/TV) together with increased trabecular thickness (Tb.Th) and trabecular number (Tb.N) (Fig. 5, *E*-G). Similarly, cortical thickness (Cortical.Th) and cortical area (Cortical B·Ar) were markedly increased (Fig. 5, H&I). The effect of Ebf1 deletion on the tibial and vertebral bone parameters were in accordance with the femur data (Supplemental Fig. 4&5). μCT analysis of the 12-week-old Ebf1$^{-/-}_{Osx}$ female mice also further supported these findings (Supplemental Fig. 6–8). Interestingly, we found that in aged male mice at 24 weeks of age deletion of Ebf1 with Osx-Cre no longer affected bone mass as measured by μCT (Supplemental table 1, Supplemental Fig. 9). We further analyzed gene expression in the total bone samples of 12- and 24-week-old Ebf1$_{Osx}$ and Ebf1$_{hOC}$ mice. We did not observe any significant difference in the expression of Ebf1 or in other osteoblast-related genes between the different genotypes (Supplemental Fig. 10). This was likely due to the presence of bone marrow in the samples, as Ebf1 is expressed also in the hematopoietic cells [13].

To further investigate the mechanisms leading to the increased bone mass in Ebf1$^{-/-}_{Osx}$ mice we performed quantitative histomorphometry. First, histomorphometric analysis confirmed the robustly increased trabecular bone mass in Ebf1$^{-/-}_{Osx}$ mice compared to controls (Fig. 6-B). Furthermore, the number of osteoblasts (N.Ob/B·Pm) and osteoblast surface (Ob.S/B·Pm) were significantly increased in the Ebf1$^{-/-}_{Osx}$ mice compared to controls, while there were no significant differences in osteoid surface (OS/BS) or osteoid thickness (O·Th) (Fig. 6-B, Table 1). These data suggested that the osteoblastic population was significantly increased in Ebf1$^{-/-}_{Osx}$ mice but osteoblast activity was not enhanced.

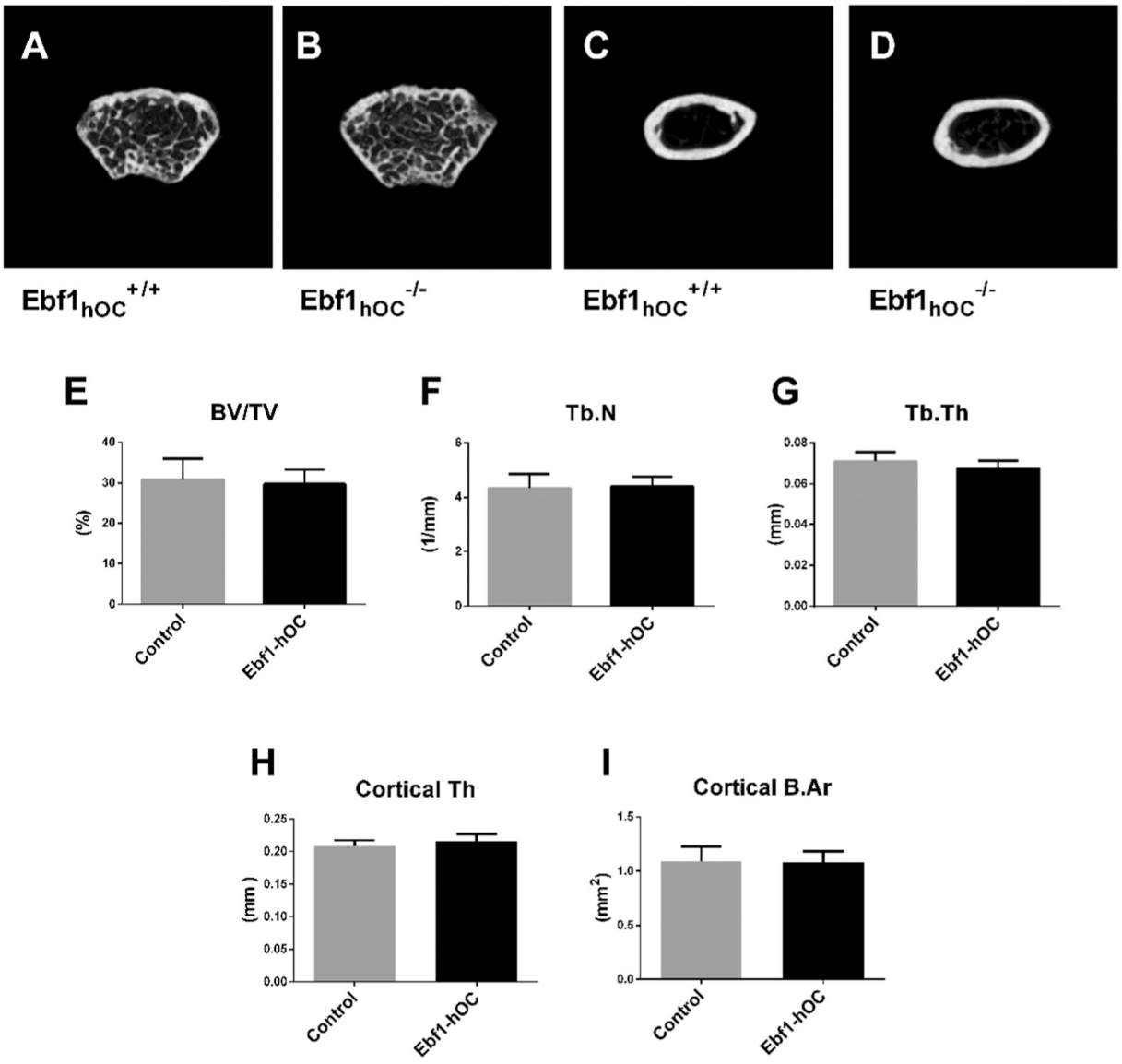

Fig. 7. Results of the femoral μCT-analysis of $Ebf1_{hOC}$ mice. 3D rendered representation of the trabecular region of interest in mice $Ebf1^{+/+}_{hOC}$(A) and $Ebf1^{-/-}_{hOC}$ mice (B) and cortical region of interest in $Ebf1^{+/+}_{hOC}$ mice (C) and $Ebf1^{-/-}_{hOC}$ mice (D). Deletion of Ebf1 in mature osteoblasts (12-week-old $Ebf1^{-/-}_{hOC}$ mice), had no effect on trabecular bone parameters (E-G) or cortical bone parameters (H and I). $n = 7$ in $Ebf1^{+/+}_{hOC}$ mice, $n = 5$ in $Ebf1^{-/-}_{hOC}$ mice.

Table 2
Histomorphometric analysis of $Ebf1^{-/-}_{hOC}$ mice.

Parameter	$Ebf1^{fl/fl}$	$Ebf1^{-/-}_{hOC}$
Tb.N [/mm]	4.05 ± 0.24	4.10 ± 0.48
Tb.Sp [um]	201 ± 9.84	192 ± 30.4
MAR [um/day]	1.60 ± 0.27	1.72 ± 0.11
BFR/BV [%/day]	2.77 ± 0.54	3.19 ± 0.86
Oc.S/B·Pm [%]	7.71 ± 2.55	9.50 ± 1.18
N.Oc/B.Pm[/mm]	3.02 ± 0.87	3.70 ± 0.60
OS/BS [%]	9.32 ± 5.43	7.85 ± 3.28
O·Th [um]	2.59 ± 0.80	2.33 ± 0.53

Data are mean ± SD.
$n = 5$ for Control, $n = 4$ $Ebf1^{-/-}_{hOC}$.

Dynamic measurements did not show any significant difference in the mineral apposition or bone formation rates (MAR or BFR/BV) between $Ebf1^{-/-}_{Osx}$ mice and control mice indicating that the osteoblast function was not affected by the loss of Ebf1 in early osteoblasts at least at this time point (Supplemental Fig. 11). The number of osteoclasts (N.Oc/B·Pm), osteoclast surface (Oc.S/BS) and eroded surface (ES, data not shown) did not differ between the groups (Table 1) indicating that osteoclastic bone resorption was not altered in $Ebf1^{-/-}_{Osx}$ mice.

Although we observed that hOC-Cre targets the Ebf1 allele (Supplemental Fig. 1-D), μCT analysis did not detect any significant differences in either trabecular or cortical bone mass in the $Ebf1^{-/-}_{hOC}$ mice femurs compared to the controls at either 12- or 24-week time points (Fig. 7, *E*-I, Supplemental table 2). Nor did we detect any significant differences between $Ebf1^{-/-}_{hOC}$ and control mice in μCT analyses of the tibia or vertebrae in males or in females (Supplemental Fig. 12–17). We examined the same histomorphometric parameters also in the $Ebf1^{-/-}_{hOC}$ mice. There were no changes in any of the studied parameters (Fig. 6-D, Table 2).

This further verified our previous results of Ebf1 not having a major role in the mature osteoblasts expressing osteocalcin.

4. Discussion

There are conflicting data on the role of Ebf1 in osteoblast

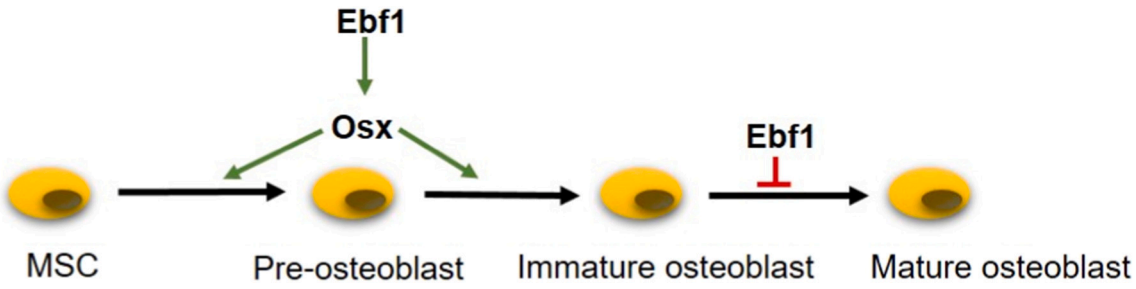

Fig. 8. Suggested model of Ebf1 function during osteoblast differentiation. Ebf1 promotes early osteoblast differentiation *via* inducing Osterix (Osx) expression, while it suppresses osteoblast function in more mature cells.

differentiation and bone formation. Hesslein et al. reported that the global deletion of Ebf1 in mice leads to increased bone formation and osteoblast differentiation, suggesting Ebf1 to function as a negative regulator of bone formation [9]. We previously reported [10] that deletion of only one Ebf1 allele is enough to increase bone volume and bone formation. Same effect was recapitulated in the Ebf1 over-expressing ColI2.3-Ebf1-mice, in which the overexpression was targeted to mature osteoblasts. ColI2.3-Ebf1-mice had significantly decreased bone volume due to low osteoblast activity, although osteoblast number was increased [10]. In some studies, Ebf1 deletion, however, had no effect on the bone phenotype. Zee et al. deleted Ebf1 in the mouse osteoblast lineage cells with Runx2-Cre [11]. These mice had normal body composition compared to controls, and no changes in the osteoblast number, bone formation rate or bone mass at 4 weeks of age. They suggested Ebf1 to function as a transcription factor regulating osteoblast differentiation in a non-cell-autonomous manner [11]. Seike et al. reported that limb bud mesenchymal cell-targeted Ebf1 deletion (Prx1-Cre;$Ebf1^{f/f}$) did not lead to any gross bone abnormalities compared to controls at 18- or 90-week-old mice [12]. Derecka et al. in turn used 8–14-week old Prx1-Cre;$Ebf1^{f/f}$ mice, in which trabecular bone volume was modestly, but significantly increased [14], which is in line with our findings in this study.

Ebf1 has been shown to have a major role in regulating the differentiation and development of multiple different cell types and tissues including the central nervous system. Indeed, the global Ebf1 knockout mice have a severe neuronal phenotype that in part leads to small body size and failure to thrive. Therefore, it is not clear whether the changes in skeletal development arise from defects in skeletal cell types or from the changes in the brain development or other metabolic effects. The age dependent changes in the bone formation activity must also be taken into account. During rapid growth molecular mechanisms regulating bone mass differ from those in older animals, as for example older mice have less transcriptional activation following mechanical loading [27]. In C57BL/6 J mice trabecular bone volume is greatest at 6–8 weeks of age and declines steadily thereafter [28]. This might explain why there was no bone phenotype in young [11], or in significantly older Ebf1 conditional knockout mice [12].

There has also been discrepancy between *in vivo* and *in vitro* results in the previous Ebf1 knockout studies. Hesslein et al. reported that in their global Ebf1 knockout model the $Ebf1^{-/-}$ osteoblasts were indistinguishable from the control cells in their proliferation ability and alkaline phosphatase expression *in vitro*, although bone formation was significantly increased in the knockout mice *in vivo*. Histologic and histomorphometric data showed significantly increased osteoblast numbers in the global knockout mice, which is most likely the reason behind the increase in osteoid and bone [9]. Zee et al. showed that $Ebf1^{-/-}$ osteoblasts formed fewer mineralized nodules and produced less alkaline phosphatase *in vitro*, while *in vivo* there was no phenotype [11]. Derecka et al. showed how their $Ebf1^{-/-}$ mice had increased trabecular bone *in vivo*, but the Ebf1 deficient cells failed to differentiate into osteoblasts *in vitro* [14]. These data are in line with our observations both *in vitro* and *in vivo*, although they did not evaluate osteoid thickness or perform dynamic histomorphometry that would have allowed for comparison of osteoblast functions between the two mouse models.

The discrepancy between the *in vivo* and *in vitro* results might also be due to other Ebfs co-operating with or compensating for Ebf1. One of the strong candidates is Ebf2, which has also been detected in osteoblast progenitors. $Ebf2^{-/-}$ mice had decreased bone mass and increased number of osteoclasts. Even though the global inactivation of Ebf2 had no great effect on the generation of osteoblasts or the bone formation rate, Ebf1 was detected in Ebf2 expressing osteoblastic cells [29]. Ebf1 and Ebf3 in turn co-operate in the maintenance of marrow cavities and hematopoietic stem cell niche formation [12,14]. Kieslinger et al. have also shown how Ebf1, Ebf2 and Ebf3 act redundantly in the support of hematopoietic cells [30]. It is therefore possible that lack of Ebf1 could be compensated for by the other Ebfs *in vivo*.

The data from our mouse models, together with data from Derecka et al., challenge the previous global and osteoblast-specific knockouts and shed more light to the role of Ebf1 in early as well as in mature osteoblasts. To overcome the challenges of the global Ebf1 knockout, we first used haploinsufficient $Ebf1^{+/-}$ mice to study the primary osteoblast differentiation *in vitro*. In our calvarial osteoblast cultures the haploinsufficient $Ebf1^{+/-}$ cells with significantly reduced Ebf1 expression had significantly impaired osteoblast differentiation and decreased expression of osteoblastic mRNAs such as ALP, Osterix, Col1a1 and Osteocalcin. Conversely, overexpression of Ebf1 led to enhanced osteoblast differentiation and elevated expression of ALP and Osterix. Similar observation was also made by Zee et al. where the overexpression of Ebf1 in MC3T3-E1 cells led to increased extracellular matrix mineralization [11]. In the Ebf1 overexpressing ColI2.3-Ebf1 mouse model the results, however, were the opposite. Despite increased osteoblast numbers *in vivo* these mice had low bone volume, mineral apposition rate and decreased bone formation rate suggesting a functional impairment in individual osteoblasts. *In vitro* the osteoblast differentiation was decreased. These data suggest that Ebf1 has opposite roles at different stages of osteoblast differentiation. In ColI2.3-Ebf1 mouse the overexpression effect is targeted into the mature osteoblasts, where it would seem to inhibit the bone accrual, whereas in our study, the overexpression of Ebf1 in the early osteoblasts drives the differentiation. Mechanistically, we found that Ebf1 directly induces Osterix expression by binding to its promoter using Osx-Luc reporter and ChIP assays, explaining at least in part the stimulation of osteoblast differentiation by Ebf1. Interestingly, Komori et al. have shown that overexpression of Osterix in mature osteoblasts results in low bone mass and spontaneous fractures similarly to Runx2 overexpression. Based on their data, Osterix is required for osteoblast differentiation but excess Osterix in mature osteoblasts inhibits normal osteoblast function [31]. These data provide a putative mechanism for the negative effect of Ebf1 overexpression in mature osteoblasts.

To study the differentiation stage specific effects further, we generated differentiation stage-targeted Ebf1 knockout mice. Our μCT results showed that the deletion of Ebf1 in the early osteoblasts in $Ebf1_{Osx}^{-/-}$ mice led to increased trabecular and cortical bone mass, while deletion in mature osteoblasts in $Ebf1_{hOC}^{-/-}$ mice did not result in bone phenotype at

either 12 or 24 weeks of age. Histomorphometric analyses of the 12-week-old $Ebf1^{-/-}_{Osx}$ demonstrated higher bone mass and increased osteoblast number and surface, although bone formation was unchanged at that time point. This might be due to the age-dependent changes in bone formation activity. Since the mice at 12-week-old are considered as skeletally mature, the bone formation activity may have already reached a plateau. This data is in accordance with data from Derecka et al. who presented modestly but significantly increased bone volume and osteoblast numbers in the trabecular bone area of Prx1-Cre;$Ebf1^{f/f}$ mice [14].

To conclude, based on our data Ebf1 promotes early osteoblast differentiation by directly inducing Osterix expression (Fig. 8). However, when osteoblast differentiation progresses to mature stage, Ebf1 suppresses bone formation similarly to Osterix [31]. Thus, its deletion in already committed, Osx-Cre expressing osteoblasts leads to increased bone mass. Based on our data and those of others Ebf1 appears to have a major role in bone formation only in young animals during growth and Ebf1 is redundant for the maintenance of bone mass in skeletally mature mice.

CRediT authorship contribution statement

Vappu Nieminen-Pihala: Investigation, Formal analysis, Data curation, Writing - Original Draft, Visualization, Validation. **Kati Tarkkonen:** Investigation, Resources, Validation. **Julius Laine:** Investigation, Resources. **Petri Rummukainen:** Investigation. **Lauri Saastamoinen:** Investigation. **Kenici Nagano:** Investigation. **Roland Baron:** Investigation. **Riku Kiviranta**: Conceptualization, Supervision, Project administration, Methodology, Funding acquisition, Writing – Review and editing.

Funding

This study was funded by the Academy of Finland (R.K.: 139165, 268535, 298625, 316800), Emil Aaltonen Foundation, Sigrid Juselius Foundation, the Finnish Cultural Foundation, Turku University Foundation and Turku Doctoral Programme of Molecular Medicine.

Acknowledgements

The authors thank Merja Lakkisto and the staff of Turku Central Animal Laboratory for their excellent technical assistance.

Appendix A. Supplementary data

Supplementary data to this article can be found online at https://doi.org/10.1016/j.bone.2021.115884.

References

[1] T. Komori, Regulation of osteoblast differentiation by transcription factors, J. Cell. Biochem. 99 (2006) 1233–1239, https://doi.org/10.1002/jcb.20958.
[2] P. Ducy, R. Zhang, V. Geoffroy, A.L. Ridall, G. Karsenty, Osf2/Cbfa1: a transcriptional activator of osteoblast differentiation, Cell. 89 (1997) 747–754. http://www.ncbi.nlm.nih.gov/pubmed/9182762. (Accessed 27 October 2016).
[3] K. Nakashima, X. Zhou, G. Kunkel, Z. Zhang, J.M. Deng, R.R. Behringer, B. de Crombrugghe, The novel zinc finger-containing transcription factor osterix is required for osteoblast differentiation and bone formation, Cell. 108 (2002) 17–29. http://www.ncbi.nlm.nih.gov/pubmed/11792318. (Accessed 27 October 2016).
[4] F. Otto, A.P. Thornell, T. Crompton, A. Denzel, K.C. Gilmour, I.R. Rosewell, G. W. Stamp, R.S. Beddington, S. Mundlos, B.R. Olsen, P.B. Selby, M.J. Owen, Cbfa1, a candidate gene for cleidocranial dysplasia syndrome, is essential for osteoblast differentiation and bone development, Cell. 89 (1997) 765–771. http://www.ncbi.nlm.nih.gov/pubmed/9182764. (Accessed 27 October 2016).
[5] W.J. Boyle, W.S. Simonet, D.L. Lacey, Osteoclast differentiation and activation, Nature. 423 (2003) 337–342, https://doi.org/10.1038/nature01658.
[6] J. Hagman, C. Belanger, A. Travis, C.W. Turck, R. Grosschedl, Cloning and functional characterization of early B-cell factor, a regulator of lymphocyte-specific gene expression, Genes Dev. 7 (1993) 760–773. http://www.ncbi.nlm.nih.gov/pubmed/8491377. (Accessed 4 August 2016).
[7] P. Akerblad, R. Månsson, A. Lagergren, S. Westerlund, B. Basta, U. Lind, A. Thelin, R. Gisler, D. Liberg, S. Nelander, K. Bamberg, M. Sigvardsson, Gene expression analysis suggests that EBF-1 and PPARgamma2 induce adipogenesis of NIH-3T3 cells with similar efficiency and kinetics, Physiol. Genomics 23 (2005) 206–216, https://doi.org/10.1152/physiolgenomics.00015.2005.
[8] S.S. Wang, J.W. Lewcock, P. Feinstein, P. Mombaerts, R.R. Reed, Genetic disruptions of O/E2 and O/E3 genes reveal involvement in olfactory receptor neuron projection, Development. 131 (2004) 1377–1388, https://doi.org/10.1242/dev.01009.
[9] D.G.T. Hesslein, J.A. Fretz, Y. Xi, T. Nelson, S. Zhou, J.A. Lorenzo, D.G. Schatz, M. C. Horowitz, Ebf1-dependent control of the osteoblast and adipocyte lineages, Bone. 44 (2009) 537–546, https://doi.org/10.1016/j.bone.2008.11.021.
[10] R. Kiviranta, K. Yamana, H. Saito, D.K. Ho, J. Laine, K. Tarkkonen, V. Nieminen-Pihala, E. Hesse, D. Correa, J. Määttä, L. Tessarollo, E.D. Rosen, W.C. Horne, N. A. Jenkins, N.G. Copeland, S. Warming, R. Baron, Coordinated transcriptional regulation of bone homeostasis by Ebf1 and Zfp521 in both mesenchymal and hematopoietic lineages, J. Exp. Med. 210 (2013) 969–985. http://www.pubmedcentral.nih.gov/articlerender.fcgi?artid=3646489&tool=pmcentrez&rendertype=abstract.
[11] T. Zee, S. Boller, I. Györy, M.P. Makinistoglu, J.P. Tuckermann, R. Grosschedl, G. Karsenty, The transcription factor early B-cell factor 1 regulates bone formation in an osteoblast-nonautonomous manner, FEBS Lett. 587 (2013) 711–716, https://doi.org/10.1016/j.febslet.2013.01.049.
[12] M. Seike, Y. Omatsu, H. Watanabe, G. Kondoh, T. Nagasawa, Stem cell niche-specific Ebf3 maintains the bone marrow cavity, Genes Dev. 32 (2018) 359–372, https://doi.org/10.1101/gad.311068.117.
[13] M. Seike, Y. Omatsu, H. Watanabe, G. Kondoh, T. Nagasawa, Stem cell niche-specific Ebf3 maintains the bone marrow cavity, Genes Dev. 32 (2018) 359–372, https://doi.org/10.1101/gad.311068.117.
[14] M. Derecka, J. Stefan Herman, P. Cauchy, S. Ramamoorthy, E. Lupar, D. Grün, R. Grosschedl, EBF1-deficient bone marrow stroma elicits persistent changes in HSC potential, Nat. Immunol. (n.d.). doi:https://doi.org/10.1038/s41590-020-0595-7.
[15] H. Lin, R. Grosschedl, Failure of B-cell differentiation in mice lacking the transcription factor EBF, Nature. 376 (1995) 263–267, https://doi.org/10.1038/376263a0.
[16] T. Treiber, E.M. Mandel, S. Pott, I. Györy, S. Firner, E.T. Liu, R. Grosschedl, Early B cell factor 1 regulates B cell gene networks by activation, repression, and transcription- independent poising of chromatin, Immunity. 32 (2010) 714–725, https://doi.org/10.1016/j.immuni.2010.04.013.
[17] S.J. Rodda, A.P. McMahon, Distinct roles for hedgehog and canonical Wnt signaling in specification, differentiation and maintenance of osteoblast progenitors, Development. 133 (2006) 3231–3244, https://doi.org/10.1242/dev.02480.
[18] M. Zhang, S. Xuan, M.L. Bouxsein, D. von Stechow, N. Akeno, M.C. Faugere, H. Malluche, G. Zhao, C.J. Rosen, A. Efstratiadis, T.L. Clemens, Osteoblast-specific knockout of the insulin-like growth factor (IGF) receptor gene reveals an essential role of IGF signaling in bone matrix mineralization, J. Biol. Chem. 277 (2002) 44005–44012, https://doi.org/10.1074/jbc.M208265200.
[19] W. Huang, B.R. Olsen, Skeletal Defects in Osterix-Cre Transgenic Mice, (n.d.). doi: https://doi.org/10.1007/s11248-014-9828-6.
[20] M.A. Jimenez, P. Akerblad, M. Sigvardsson, E.D. Rosen, Critical role for Ebf1 and Ebf2 in the Adipogenic transcriptional Cascade, Mol. Cell. Biol. 27 (2007) 743–757, https://doi.org/10.1128/mcb.01557-06.
[21] Y. Nishio, Y. Dong, M. Paris, R.J. O'Keefe, E.M. Schwarz, H. Drissi, Runx2-mediated regulation of the zinc finger Osterix/Sp7 gene, Gene. 372 (2006) 62–70, https://doi.org/10.1016/j.gene.2005.12.022.
[22] P. Östling, J.K. Björk, P. Roos-Mattjus, V. Mezger, L. Sistonen, Heat shock factor 2 (HSF2) contributes to inducible expression of hsp genes through interplay with HSF1, J. Biol. Chem. 282 (2007) 7077–7086, https://doi.org/10.1074/jbc.M607556200.
[23] D.W. Dempster, J.E. Compston, M.K. Drezner, F.H. Glorieux, J.A. Kanis, H. Malluche, P.J. Meunier, S.M. Ott, R.R. Recker, A.M. Parfitt, Standardized nomenclature, symbols, and units for bone histomorphometry: a 2012 update of the report of the ASBMR Histomorphometry nomenclature committee, J. Bone Miner. Res. 28 (2013) 2–17, https://doi.org/10.1002/jbmr.1805.
[24] S.-L. Cheng, J.-S. Shao, N. Charlton-Kachigian, A.P. Loewy, D.A. Towler, MSX2 promotes osteogenesis and suppresses adipogenic differentiation of multipotent mesenchymal progenitors, J. Biol. Chem. 278 (2003) 45969–45977, https://doi.org/10.1074/jbc.M306972200.
[25] M.-H. Lee, T.-G. Kwon, H.-S. Park, J.M. Wozney, H.-M. Ryoo, BMP-2-induced Osterix expression is mediated by Dlx5 but is independent of Runx2, Biochem. Biophys. Res. Commun. 309 (2003) 689–694, https://doi.org/10.1016/j.bbrc.2003.08.058.
[26] J.S. Park, W.Y. Baek, Y.H. Kim, J.E. Kim, In vivo expression of Osterix in mature granule cells of adult mouse olfactory bulb, Biochem. Biophys. Res. Commun. 407 (2011) 842–847, https://doi.org/10.1016/j.bbrc.2011.03.129.
[27] C.J. Chermside-Scabbo, T.L. Harris, M.D. Brodt, I. Braenne, B. Zhang, C.R. Farber, M.J. Silva, Old mice have less transcriptional activation but similar periosteal cell proliferation compared to young-adult mice in response to in vivo mechanical loading, J. Bone Miner. Res. 35 (2020) 1751–1764, https://doi.org/10.1002/jbmr.4031.
[28] V. Glatt, E. Canalis, L. Stadmeyer, M.L. Bouxsein, Age-related changes in trabecular architecture differ in female and male C57BL/6J mice, J. Bone Miner. Res. 22 (2007) 1197–1207, https://doi.org/10.1359/jbmr.070507.

[29] M. Kieslinger, S. Folberth, G. Dobreva, T. Dorn, L. Croci, R. Erben, G.G. Consalez, R. Grosschedl, EBF2 regulates osteoblast-dependent differentiation of osteoclasts, Dev. Cell 9 (2005) 757–767, https://doi.org/10.1016/j.devcel.2005.10.009.
[30] M. Kieslinger, S. Hiechinger, G. Dobreva, G.G. Consalez, R. Grosschedl, Early B cell factor 2 regulates hematopoietic stem cell homeostasis in a cell-nonautonomous manner, Cell Stem Cell. 7 (2010) 496–507, https://doi.org/10.1016/j.stem.2010.07.015.
[31] C.A. Yoshida, H. Komori, Z. Maruyama, T. Miyazaki, K. Kawasaki, T. Furuichi, R. Fukuyama, M. Mori, K. Yamana, K. Nakamura, W. Liu, S. Toyosawa, T. Moriishi, H. Kawaguchi, K. Takada, T. Komori, Sp7 inhibits osteoblast differentiation at a late stage in mice, PLoS One. 7 (2012), https://doi.org/10.1371/journal.pone.0032364.